Formation energies of group I and II metal oxides using random phase approximation

Jun Yan, Jens S. Hummelshøj, and Jens K. Nørskov

Phys. Rev. B **87**, 075207 — Published 25 February 2013

DOI: 10.1103/PhysRevB.87.075207

Formation Energies of Group I, II Metal Oxides using Random Phase Approximation

Jun Yan,[1,*] Jens S. Hummelshøj,[1] and Jens K. Nørskov[1,2]

[1]*SUNCAT Center for Interface Science and Catalysis, SLAC National Accelerator Laboratory, 2575 Sand Hill Road, Menlo Park, CA 94025, USA*

[2]*Department of Chemical Engineering, Stanford University, Stanford, CA 94305, USA*

(Dated: January 16, 2013)

The enthalpy of formation for 23 metal oxides, which include group I and II as well as two transition metals (Ti and Ru), are calculated using random phase approximation (RPA). Compared to PBE xc-functional, RPA reduces the mean absolute error (MAE) per oxygen from 0.44 eV to 0.15 eV. The calculated deviations with experiments are seperated into two parts: a systematic and uniform error related to the reference energy of O and the ones specific to diffferent oxidation states O^{2-}, O_2^{2-}, O_2^-. Our results show that RPA improves both the reference energy, although the error is not completely eliminated, and simultaneously over the three oxidation states.

PACS numbers: 71.15.-m, 71.15.Mb, 71.15.Nc

I. INTRODUCTION

Oxides are widely used in industrial heterogeneous catalysis, photo catalysis, electrochemistry and as electrode materials in batteries and fuel cells. To facilitate the computational engineering and design of novel materials in these fields, it is vitally important to be able to quantitatively predict the formation/reactions energies of oxides, with the goal of achieving chemical precision (1 kcal/mol, or 43 meV). LDA/GGA, the success of which has largely relied on the mysterious error cancellation in the exchange-correlation term[1], generally fails for these oxides, showing systematic and non-canceling errors. In particular, the formation energies of oxides are systematically underestimated with GGA[2]. This has been largely attributed to the well known overbinding of the O_2 gas phase molecule with GGA. By defining the binding energy of O_2 through the electrochemical formation of a gas phase water molecule from O_2 and H_2[3], the problem of overbinding the O_2 molecule and thus underbinding the oxides is largely cured[4]. Such a scheme, however, provides a constant shift of the formation energies without taking into account the difference among distinct oxidation states such as oxides (O^{2-}), peroxides (O_2^{2-}), superoxides (O_2^-).

Recently, the use of exact exchange (EXX), plus correlation energy from Random Phase Approximation (RPA) has emerged as a promising approach to obtain non-empirical exchange-correlation terms[5–11]. EXX is free of self-interaction error, while the RPA correlation energy takes into account dynamic electronic screening and is fully non-local. EXX+RPA has been shown to systematically improve lattice constants[12], atomization/cohesive energies[13,14], adsorption energies[15–17] and reaction barriers[18] for a wide range of systems that have ionic, covalent and van der Waals (vdW) interactions. In particular, by summing up the ring diagrams in many body perturbation theory, RPA takes into account the long range density fluctuations and is especially suitable for vdW bonded systems[19,20]. For example, graphite[21], which has vdW interlayer coupling, graphene adsorbed on metal surfaces[22], which have mixed vdW and covalent bonds, and the S22 molecule set[18], which consists of molecules containing hydrogen bonds, dispersion bonds and mixed bonds, are all significantly improved with RPA compared to PBE xc-functional. On the other hand, it is reported that RPA does slightly worse than PBE in reproducing the atomization energies of molecules, for example the G2-I set[18], and the cohesive energies for 24 representative solids[12], which consists of ionic crystal, semiconductors and metals, even though the lattice constants and bulk moduli of these solids calculated with RPA agree better with experiments than PBE.

In this paper, we apply the EXX+RPA approach to benchmark the formation energies of group I and II metal oxides as well as two transition metal oxides (TiO_2 and RuO_2). Our results show that EXX+RPA formation energies improve over PBE and reduce the overall mean absolute error (MAE). Such improvement is further separated into two parts: the better description of the oxygen reference energy and the simultaneously improvement over three oxidation states O^{2-}, O_2^{2-}, O_2^-.

II. METHOD AND COMPUTATIONAL DETAILS

A. EXX+RPA scheme

We adopted the scheme of calculating the EXX+RPA total energies non-self-consistently. Self-consistent RPA calculations have only been reported in the case of obtaining the RPA correlation potential for dissociation of small molecules[23]. Under the non-self-consistent scheme, the EXX+RPA total energies are expressed as

$$E^{\mathrm{EXX}} = E^{\mathrm{tot}}_{(\mathrm{semi})\mathrm{loc}} - E^{\mathrm{xc}}_{(\mathrm{semi})\mathrm{loc}} + E^{\mathrm{x}}_{\mathrm{exx}}, \quad (1)$$

$$E^{\mathrm{EXX+RPA}} = E^{\mathrm{EXX}} + E^{\mathrm{c}}_{\mathrm{rpa}}. \quad (2)$$

where a self-consistent calculation is performed with a (semi-)local xc-functional to get the total energy $E^{\mathrm{tot}}_{(\mathrm{semi})\mathrm{loc}}$ and the xc contribution to the energy $E^{\mathrm{xc}}_{(\mathrm{semi})\mathrm{loc}}$,

followed by a non-self-consistent calculation to obtain the exact exchange $E_{\rm exx}^{\rm x}$ and the RPA correlation energy $E_{\rm rpa}^{\rm c}$. The latter is formulated as

$$E_{\rm rpa}^{\rm c} = \int_0^\infty \frac{d\omega}{2\pi} {\rm Tr}\{\ln[1 - v\chi^0(i\omega)] + v\chi^0(i\omega)\}, \quad (3)$$

where v is the Coulomb interaction kernel and χ^0, the non-interacting response function, is evaluated in a plane wave basis using 'sum of state' approach written as

$$\chi^0_{\mathbf{GG'}}(\mathbf{q}, i\omega) = \frac{1}{\Omega} \sum_{\mathbf{k}}^{\rm BZ} \sum_{\sigma nn'} \frac{f_{\sigma n\mathbf{k}} - f_{\sigma n'\mathbf{k+q}}}{i\omega + \epsilon_{\sigma n\mathbf{k}} - \epsilon_{\sigma n'\mathbf{k+q}}} \quad (4)$$
$$\times \langle \psi_{\sigma n\mathbf{k}} | \, e^{-i(\mathbf{q+G})\cdot\mathbf{r}} \, | \psi_{\sigma n'\mathbf{k+q}} \rangle \langle \psi_{\sigma n'\mathbf{k+q}} | \, e^{i(\mathbf{q+G'})\cdot\mathbf{r}} \, | \psi_{\sigma n\mathbf{k}} \rangle .$$

The occupation $f_{\sigma n\mathbf{k}}$, KS eigenvalue $\epsilon_{\sigma n\mathbf{k}}$ and eigenstate $\psi_{\sigma n\mathbf{k}}$ for band n at wave vector $\mathbf{k}$ with spin σ are extracted from the previous self-consistent calculation. For details on the implementation of the response function and the RPA method, refer to Ref. 24 and 25.

Since our EXX and RPA calculations are performed non-self-consistently, it is important to choose reliable starting structures, xc-functional and orbitals. The influence of difference xc-functionals (LDA, PBE, or even PBE0) and orbitals (Kohn-Sham or Hartree-Fock) on non-self-consistent RPA correlation energies are discussed extensively in the literature[12,17,19,26]. In general, the dependence of physical quantities such as lattice parameters, atomization energies, on the initial xc-functional is rather small; on the other hand, to replace Kohn-Sham orbitals using Hartree-Fock ones in the EXX and RPA calculations is reported to improve the binding energies of some molecules while worsen the others[26]. In this paper, we choose the most widely used scheme: PBE xc-functional with Kohn-Sham orbitals, despite the fact that LDA can also in many cases produce very good formation energies for metal oxides[27]. In terms of lattice parameters and atomic structures, RPA is reported to improve over PBE lattice parameters slightly for 24 representative solids[12]. We have checked that the differences in energies between the PBE and experimental lattice constants for metals are neglectable. In Section. II C, we show that for Li_2O and Cs_2O, the EXX+RPA volume can lower the total energy (per oxygen) by 5 and 44 meV, respectively, compared to the energy obtained with PBE volumes. For other more complicated oxides, the degree of freedom is much larger than its corresponding bulk metal, we were only be able to verify that in NaO_2, the differences introduced by varying the lattice parameters and the Na-O bond length are neglectable. In the following EXX+RPA calculations, we shall use PBE structures for all the oxides, metals and O_2 molecule, and focus on the performance of EXX+RPA despite all the approximations and assumptions elaborated above.

B. Criteria for choosing oxides

Since our EXX and RPA calculations are based on PBE structures, eigen energies and orbitals, the first criterion for choosing oxides is that we have reliable PBE results. Our results are obtained with GPAW, an electronic structure package employing projector augmented wave (PAW) method and three-dimensional uniform grids as well as plane wave basis. They are compared with the MaterialsProject database[28,29], which is produced with the VASP package, another electronic structure code also using PAW and plane wave basis. The difference in these two PAW implementations might be different valence states included in the PAW potential and different cutoff raidus employed for each valence state. We found that the formation energies, in particular for transition metal oxides, depend sensitively on the PAW potential used. For example, our calculated PBE formation energies (in eV) differ by 0.27 (Cu_2O), 0.14 (CuO), 0.17 (ZnO) and -0.20 (NbO_2) compared to the MaterialsProject database. Considering that the uncertainty in energies (largely due to different PAW potentials) on the PBE level of around 0.2 eV is similar to the mean average error (will shown later) we found for RPA calculations on group I, II metal oxides, we exclude the above four transition metal oxides in our RPA datasets. The oxides presented here mostly agree within 0.05 eV with the MaterialsProject database for formation energies; except that for LiO_2, the MaterialsProject database only has an unstable structure (with formation energy > 0) available and for BeO, our PBE formation energy is larger (less negative) by 0.11 eV than the database.

The second criterion in choosing a certain oxide is that a Hubbard U term is not required to get meaningful atomic structures or spin configurations. This is due to that the Hubbard U term applied to a metal oxide can not be applied to its corresponding bulk metal. An alternative way to obtain a meaningful U term for metals are proposed in the literature[30], it is however, out of scope of current work. The second criterion thus excludes $3d$ transition metal oxides such as VO and NiO. The third criterion in selecting oxides is that the calculation of the RPA correlation energy can converge within 0.05 eV meanwhile be computationally affordable, since RPA is computationally extreme demanding and scales with $O(N^4)$, where N is number of electrons in the system. Finally, experimental formation enthalpies shall be available for comparison.

Combining all the above criteria, we chose 23 metal oxides, which majorly consist of group I and II metal oxides and two transition metal oxides (TiO_2 and RuO_2).

C. Bulk volumes with EXX+RPA

In this subsection, we examine using EXX+RPA the bulk volumes and their influences on the total energies of two representative oxides: Li_2O and Cs_2O, which accord-

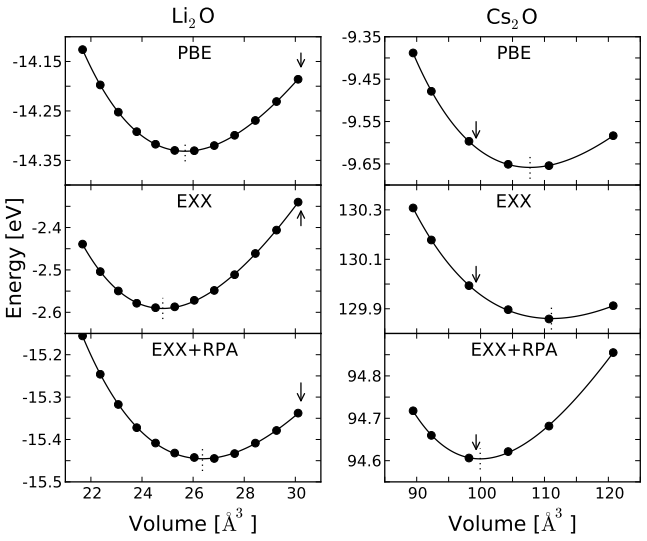

FIG. 1: Equation of state plot for Li_2O (left) and Cs_2O (right) using PBE, EXX and EXX+RPA. The EXX and RPA calculations are performed non-self-consistently on top of PBE energies and orbitals. The calculated and the experimental volumes are marked with the dashed lines and arrows, respectively.

ing to Ref.[29] have negative and positive errors of -16.3% and 16.4%, respectively, in terms of PBE volumes compared to their coresponding experimental ones. For the other 21 oxides, the errors range from -3% to 6%, with positive number corresponds to larger PBE volume compared to the experimental one.

Figure 1 shows the equation of state fit of the bulk volumes for Li_2O and Cs_2O. The details on the computation can be found in Sec. II D. For Li_2O, our PBE result underestimates the volume by 15.0% compared to experiment. EXX further shifts the minimum to lower volume with -17.9% error. Inclusion of RPA (the left bottom panel) correlation shifts the minimum to higher volume and improves slightly over PBE volume, showing an error of -12.8%. On the opposite, for Cs_2O, our PBE result overestimates the volume by 8.5 %, which is better by 7.9 % (with respect to experimental volume) than found in Ref. 29. EXX further overestimates the volume by 11.9%; and EXX+RPA improves significantly the volume with an error of only 0.6%.

Compared to use PBE volumes in EXX+RPA calculations, the EXX+RPA volumes lower the EXX+RPA total energies by 5 and 44 meV for Li_2O and Cs_2O, respectively. Since Li_2O and Cs_2O represent two extreme cases among the 23 oxides with the largest negative and positive deviations from experimental volumes, we expect that for the other 21 oxides, the differences in total energies by using PBE and EXX+RPA lattice parameters are less. It thus justifies our choices of PBE structures for all the subsequent calculations.

TABLE I: Summary of key parameters for EXX and RPA calculations: the material ID in Ref.29 (column 'ID'), the valence states included in the PAW potential (column 'Valence'), whether its spin polarized calculation (column 'Spin'), the energy cutoff $E_{\rm cut}^{\rm EXX}$ (in eV) and the number of k-points $k^{\rm EXX}$ for EXX calculations; the energy range (column $E_{\rm cut}^{\rm RPA}$, eV) for interpolation to $E_{\infty}^{\rm RPA}$ and the number of k-points $k^{\rm RPA}$ for RPA calculations. The single k-point number indicates uniform k-points in the x, y, z direction.

	ID	Valence	Spin	$E_{\rm cut}^{\rm EXX}$	$k^{\rm EXX}$	$E_{\rm cut}^{\rm RPA}$	$k^{\rm RPA}$
Li	135	2s	F	600	16	150-400	8
Li_2O	553090		F	900	16	250-400	4
Li_2O_2	841		F	900	14	250-400	4
LiO_2			T	900	14	250-400	4
Na	127	3s	F	600	16	150-400	10
Na_2O	2352		F	900	14	250-400	4
Na_2O_2	2340		F	900	14	250-400	4
NaO_2	1901		T	900	14	250-400	(6,4,6)
K	58	3s3p4s	F	700	16	250-350	10
K_2O	971		F	900	14	280-380	8
K_2O_2	28206		F	900	14	280-380	(5,5,3)
KO_2	1866		T	900	14	250-350	(6,6,4)
Rb	70	4s4p5s	F	900	16	280-380	8
Rb_2O	1394		F	900	14	280-380	6
Rb_2O_2	7895		F	900	14	280-380	(6,4,4)
RbO_2	12105		T	900	14	280-380	(6,6,4)
Cs	1	5s5p6s	F	800	16	280-380	10
Cs_2O	7988		F	900	14	280-380	(6,6,4)
Cs_2O_2	7896		F	900	14	280-350	(5,3,3)
CsO_2	1441		T	900	14	280-380	4
Be	87	2s	F	900	16	250-350	(12,12,8)
BeO	2542		F	900	14	280-380	
Mg	153	2s2p3s	F	900	16	250-400	10
MgO	1265		F	900	16	280-400	8
Ca	132	3s3p4s	F	900	16	250-350	10
CaO	2605		F	900	16	280-380	8
CaO_2			F	900	14	280-380	(6,4,6)
Sr	19999	4s4p5s	F	900	16	250-350	8
SrO	2472		F	900	14	280-380	4
Ba	122	5s5p6s	F	900	16	250-350	8
BaO	1342		F	900	14	280-380	4
Ti	72	3s3p3d4s	F	900	20	250-400	(10,10,6)
TiO_2	1203		F	900	14	280-380	(4,4,6)
Ru	33	4s4p4d5s	F	900	16	280-380	(10,10,8)
RuO_2	9449		F	900	16	280-380	(4,4,6)

D. Computational parameters

All calculations were performed with GPAW[24,33,34], an electronic structure code using the projector augmented wave method and supports basis functions such as uniform real space grids, localized atomic orbitals and plane

wave basis set. The structure relaxations were performed with the PBE xc-functional and the obtained PBE lattice parameters were used for all the subsequent PBE, EXX and RPA total energy calculations. The ground state calculations were carried out using 600 eV cutoff energy with the plane wave basis set. For EXX and RPA calculations, Table I summarizes the key parameters. For the exact exchange energy a cutoff of 900 eV was employed for most of the calculations. The divergence of the Coulomb interaction ($1/|\mathbf{q}|$ in the plane wave basis) at $\mathbf{q}=0$ was approximated following Ref. 35. Very dense k-point sampling of $16\times16\times16$ and $14\times14\times14$ were used for metals and their oxides, respectively, so that the imprecise contribution from the $\mathbf{q}=0$ can be neglected. For the EXX calculation of the gas phase O_2 molecule, a real-space implementation of the exact exchange energy was used[36] to avoid the divergence of the coulomb kernel at $\mathbf{q}=0$. Similar to the calculation of EXX, the RPA correlation energy depends largely on the cutoff energy $E^{\chi}_{\rm cut}$ (or the number of G vectors) used for the response function in Eq. (4) and the absolute convergence with respect to the cutoff energy is hard to achieve. It is, however, shown that[13,32] the electronic response at high energy cutoff is free electron-like, thus the RPA correlation energy follows a linear relation, derived from homogenous electron gas, with regards to $(E^{\chi}_{\rm cut})^{-1.5}$. Following the above scheme, each of the RPA correlation energy at E^{χ}_{∞} was extracted by performing a linear fitting using five correlation energies obtained with energy cutoff range shown in the column $E^{\rm RPA}_{\rm cut}$ in Table I. The number of bands included in the response function was set to be equal to the number of $\mathbf{G}$ vectors for a given cutoff energy. Differ from the EXX, the divergence at $\mathbf{q}=0$ for the response function was eliminated using the second order $k\cdot p$ perturbation theory[24]. As a result, much less k-points can be used for RPA calculations. The k-point sampling were carefully checked for each bulk metal and its corresponding oxides to ensure the convergence of the RPA correlation energies to be within 50 meV. Depending on the size of the unit cell, $4\times4\times4$ up to $10\times10\times10$ Monkhorst-pack k-points were used for the RPA calculations as shown in Table I. Finally, the zero point energy (ZPE) contribution to the formation energies, calculated using harmonic approximation with PBE, is applied to all the oxides, bulk metals and the O_2 molecule, and to all PBE, EXX and EXX+RPA calculations[41].

The formation energies we present in the following are obtained per oxygen atom, calculated through

$$\Delta E_{\rm O} = \frac{1}{y}E(\mathrm{A}_x\mathrm{O}_y) - \frac{x}{y}E(\mathrm{A}) - \frac{1}{2}E(\mathrm{O}_2), \qquad (5)$$

where $E(\mathrm{A}_x\mathrm{O}_y)$ and $E(\mathrm{A})$ are the total energies for the oxide $\mathrm{A}_x\mathrm{O}_y$ and the metal A, respectively, in their solid phases, and $E(\mathrm{O}_2)$ is the energy of the gas phase O_2 molecule.

TABLE II: Atomization energies of O_2 calculated using PBE, EXX only, RPA only and EXX+RPA. EXX and RPA energies were obtained on top of PBE bond length and orbitals. Spin polarized calculations were performed. The calculated results are compared with experiment[31] and previously calculated data[13,32].

		PBE	EXX	RPA	EXX+RPA	Expt.[a]
O_2	Ours	6.25	1.10	3.82	4.92	5.25
	Ref. 13	6.24	1.08	3.82	4.90	
	Ref. 32	6.20	1.08	3.82	4.90	

[a]Reference 31

III. RESULTS AND DISCUSSIONS

Before presenting the formation energies of oxides, first we discuss the binding energies of the O_2 gas phase molecule using different xc schemes. As shown in Table II, PBE significantly overbinds the O_2 molecule, giving an atomization energy of 6.25 eV compared to the experimental value of 5.25 eV. Both the exact exchange energy (column EXX) and RPA correlation energy (column RPA) contribute significantly to the atomization energies. The EXX+RPA atomization energy of 4.92 eV agrees with previous calculations from Furche[13] and Kresse et. al[32], but underbinds compared to experiment[31]. Such underbinding using EXX+RPA method is generally found for other molecules as well[18].

Figure 2 and Table III show the calculated formation energies per oxygen atom. The experimental enthalpy of formation at both zero (T=0) and room temperature (RT) are presented. The heat capacity contribution to the formation energy is around 0.01 - 0.07 eV, and is not taken into account in our calculations. The calculated

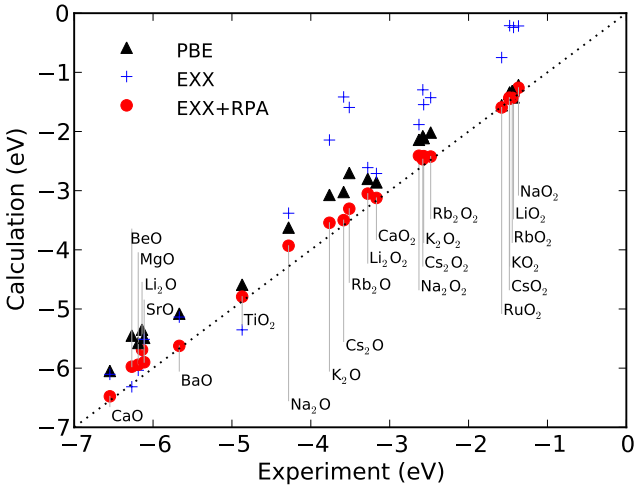

FIG. 2: (Color online) Calculated formation energies of oxides in Table III using PBE (triangles), EXX only (pluses) and EXX+RPA (circles). The dotted line indicates where calculation and experiment results coincide.

TABLE III: Formation energies (per oxygen, in eV) calculated using PBE, EXX, and EXX+RPA. EXX and RPA calculations were obtained on top of PBE structure, eigen energies and orbitals. Spin polarized calculations were performed for superoxides NaO_2, KO_2, LiO_2, RbO_2 and CsO_2. The calculated results are compared with experimental data at both room temperature (RT) and zero temperature (T=0), if available. The mean absolute error (MAE, in eV) is summarized at the end. The "MAE" and "MAE-s" term represent the MAE without and with shifting the O reference energy by 0.44 (PBE) and 0.14 (EXX+RPA) eV, respectively.

	PBE	EXX	EXX+RPA	Expt	
			@ PBE	T=0	RT
Li_2O	-5.35	-5.72	-5.69	-6.14	-6.21[a]
Li_2O_2	-2.80	-2.61	-3.05	-	-3.28[a]
LiO_2	-1.42	-0.24	-1.38	-	-1.37 to -1.50[b]
Na_2O	-3.62	-3.38	-3.93	-4.28	-4.33[a]
Na_2O_2	-2.14	-1.88	-2.41	-2.63	-2.66[a]
NaO_2	-1.22	-0.22	-1.26	-1.37	-1.35[a]
K_2O	-3.07	-2.14	-3.54	-	-3.76[a]
K_2O_2	-2.11	-1.55	-2.42	-	-2.57[a]
KO_2	-1.34	-0.21	-1.45	-1.48	-1.47[a]
Rb_2O	-2.70	-1.59	-3.30	-	-3.51[c]
Rb_2O_2	-2.02	-1.43	-2.42	-	-2.48[c]
RbO_2	-1.31	0.12	-1.43	-	-1.45[c]
Cs_2O	-3.02	-1.42	-3.50	-	-3.58[c]
Cs_2O_2	-2.08	-1.30	-2.47	-	-2.58[c]
CsO_2	-1.36	0.15	-1.43	-	-1.48[c]
BeO	-5.45	-6.31	-5.89	-6.27	-6.31[a]
MgO	-5.57	-6.04	-5.94	-6.19	-6.23[a]
CaO	-6.05	-6.10	-6.48	-6.55	-6.58[a]
CaO_2	-2.86	-2.71	-3.12	-	-3.17[e]
SrO	-5.49	-5.51	-5.90	-6.11	-6.14[a]
BaO	-5.08	-5.14	-5.62	-5.67	-5.68[a]
TiO_2	-4.59	-5.35	-4.79	-4.87	-4.90[a]
RuO_2	-1.56	-0.75	-1.59	-	-1.58[d]
MAE	0.44	0.96	0.15		
MAE-s	0.21		0.10		

[a]Reference 31
[b]Reference 37
[c]Reference 38
[d]Reference 39
[e]Reference 40

data is compared to the T=0 experimental data if available, otherwise RT data is used. Among these oxides, only MgO was calculated using EXX+RPA before, with a formation energy of 5.98 eV[11], which agrees very well with our data (5.94 eV). Table III shows that, PBE (the second column) significantly overestimates the formation energies, by up to 0.86 eV and a MAE of 0.44 eV. EXX alone (the third column) performs much worse with a MAE of 0.96 eV, and the deviations have random sign. As shown in the fourth column, inclusion of RPA correlation systematically improves the formation energy for all the oxides compared to PBE data, showing a MAE of 0.15 eV per oxygen. This is in contrast to the situation that EXX+RPA performs slightly worse than PBE for the cohesive energies of 24 representative solids[12] and atomization energies for molecules including G2-I set[18].

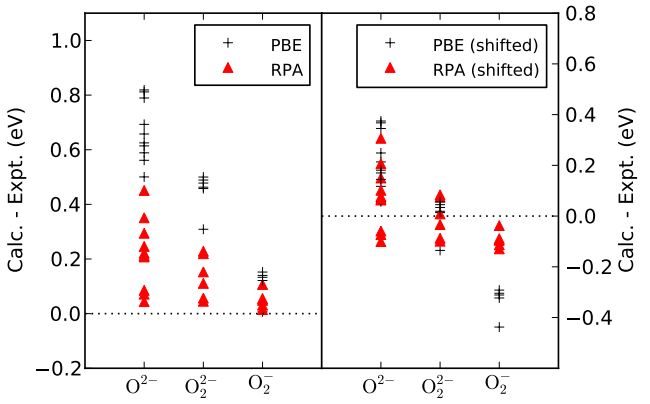

FIG. 3: (Color online) The deviations in calculated formation energies with respect to experiments, using (a) PBE (black crosses) and EXX+RPA (red triangles), (b) PBE (shifted by 0.44 eV/O) and EXX+RPA (shifted by 0.14 eV/O), as a function of different oxidation states. The 'RPA' in the figure legend corresponds to 'EXX+RPA'.

The improvement with EXX+RPA on the formation energies can be largely attributed to the better description of the O_2 molecule as reference energy, although EXX+RPA underbinds the O_2 molecule, meanwhile systematically overestimates the formation energy. By introducing a shift of 0.44 (PBE) and 0.14 (EXX+RPA, eV per oxygen atom), obtained by linear fitting to the data, in the O reference energy, the MAEs can reduce from 0.21 and 0.10 eV, shown in the bottom of Table III, for PBE and EXX+RPA calculations, respectively. Such a scheme of shifting reference energy is extensively used in DFT calculations of oxides[4], however, it provides only a constant shift in formation energies for all oxides without distinguishing different oxidation states.

In order to distinguish the effect on the reference energy and the corrections specific to different oxidiation states, in Fig. 3 we categorize group I and II oxides into three oxidation states and show the calculated deviations from experimental formation enthalpies. Shown in panel (a), without shifting the O_2 reference energy, PBE describes oxides (O^{2-}) the worst , peroxide (O_2^{2-}) better, and give good formation energies for superoxides (O_2^-). Based on the wrong O_2 reference energy, the success of PBE for superoxides could be due to the error cancellation in describing O_2 and superoxides. The trend that oxides (O^{2-}) deviate from the experiments the most, peroxides (O_2^{2-}) less and superoxides (O_2^-) the least, doesn't change from PBE to EXX+RPA. It is hard to identify whether this is due to insufficient description of the correlation with RPA for different oxidation states, or it is

merely due to the non-self consistent EXX+RPA@PBE scheme used.

After introducing the shift in the reference energy, shown in panel (b), the formation energies of oxides and peroxides improve while the ones for the superoxides worsen. On the other hand, EXX+RPA improves over PBE (shifted) for all three oxidation states. The simultaneous improvement over different oxidation states is in agreement with reports that EXX+RPA scheme work well for a variety of bonding types, including hydrogen, ionic, covalent, vdW and mixed bonds for crystals, molecules and adsorbate on surfaces[5,15,18].

Table IV summarizes the MAEs for the metals with three oxidation states (column 2-4), as well as the overall MAE for group I, II metal oxides (column 5). The two transition metal oxides are not included. EXX+RPA improves the O reference energy, but does not completely eliminate the error. By shifting the reference energy, the MAE improves for oxides and peroxides, but becomes worse for superoxides, in both PBE and EXX+RPA calculations.

We have discussed above the improvement of EXX+RPA for group I and II metal oxides, in the following we would like to comment on transition metal oxides (TMOs). Since most of the industrially applied oxides are based on transition metals, it is much more important and interesting to investigate the effect of EXX+PRA on the energetics of these oxides. The complexity of calculating the TMOs using EXX+RPA lies not only in the computational challenge, since RPA scales with $O(N^4)$, but also how to get a better initial atomic structures and electronic structures as input for EXX and RPA calculations. The complexity is further fueled by the fact that different pseudopotentials or PAW potentials can change the total energies of metal oxides on the GGA level by as large as 0.5-1 eV[42]. The error related to the uncertainties in the electron-ion interaction potential transfers itself to EXX and RPA calculations seem to be larger than the MAE error we claimed here for the group I, II metal oxides. As a result, we excluded the Cu_2O, CuO, ZnO and NbO_2 in our dataset and include only TiO_2 and RuO_2, the PBE formation energies of the latter two agree less than 0.05 eV with the MaterialsProject database. For these two TMOs, the improvement of EXX+RPA over PBE on the formation energies is rather small: 0.2 eV for TiO_2 and almost no improvement for RuO_2.

TABLE IV: A summary of the mean absolute errors (MAE, in eV) without and with shifted O reference energy (0.44 and 0.14 eV/O for PBE and EXX+RPA, respectively), calculated with PBE and EXX+RPA for group I, II metal with different oxidation states: O^{2-}, O_2^{2-}, O_2^- and their overall MAEs. The MAE for the transition metal oxides is shown in the last column. The 'RPA' in the table is actually 'EXX+RPA'.

	O^{2-}	O_2^{2-}	O_2^-	overall
PBE	0.67	0.45	0.11	0.47
PBE (shifted)	0.22	0.05	0.33	0.20
RPA	0.22	0.14	0.05	0.15
RPA (shifted)	0.12	0.06	0.09	0.10

IV. CONCLUSIONS

In conclusion, we have calculated the formation energies of group I and II metal oxides and a few transition metal oxides using exact exchange and correlation from random phase approximation. The EXX+RPA method improves over PBE functional and reduce the MAE from 0.44 eV (PBE) to 0.15 eV (EXX+RPA). The improvement is separated into two parts: the systematic better description of the O reference energy and the simultaneous improvement over the three oxidation state O^{2-}, O_2^{2-}, O_2^-.

V. ACKNOWLEDGEMENTS

J. Y. acknowledges Alan Luntz for suggesting the project, Marcin Dułak for insights on the PAW potentials, and Paweł Zawadzki for providing the energy of the O_2 molecule with the VASP package. The authors acknowledge support by the Department of Energy, Office of Basic Energy Sciences, under contract DE-AC02-76SF00515. This work partially ($\sim 50\%$) used the Extreme Science and Engineering Discovery Environment (XSEDE), which is supported by National Science Foundation grant number OCI-1053575.

* Electronic address: junyan@stanford.edu

[1] A. J. Cohen, P. Mori-Sánchez, and W. Yang, Chem. Rev. **112**, 289 (2012).
[2] L. Wang, T. Maxisch, and G. Ceder, Phys. Rev. B **73**, 195107 (2006).
[3] J. K. Nørskov, J. Rossmeisl, A. Logadottir, L. Lindqvist, J. R. Kitchin, T. Bligaard, and H. Jónsson, J. Phys. Chem. B **108**, 17886 (2004).
[4] J. I. Martínez, H. A. Hansen, J. Rossmeisl, and J. K. Nørskov, Phys. Rev. B **79**, 045120 (2009).
[5] A. Heßelmann and A. Görling, Molecular Physics **109**, 2473 (2011).
[6] H. Eshuis, J. E. Bates, and F. Furche, Theor. Chem. Acc. **131**, 1084 (2012).
[7] J. Paier, X. Ren, P. Rinke, G. E. Scuseria, A. Grüneis, G. Kresse, and M. Scheffler, New J. Phys. **14**, 043002 (2012).
[8] M. Fuchs and X. Gonze, Phys. Rev. B **65**, 235109 (2002).
[9] F. Aryasetiawan, T. Miyake, and K. Terakura, Phys. Rev. Lett. **88**, 166401 (2002).
[10] G. E. Scuseria, T. M. Henderson, and D. C. Sorensen, J. Chem. Phys. **129**, 231101 (2008).
[11] J. Harl and G. Kresse, Phys. Rev. Lett. **103**, 056401 (2009).
[12] J. Harl, L. Schimka, and G. Kresse, Phys. Rev. B **81**, 115126 (2010).
[13] F. Furche, Phys. Rev. B **64**, 195120 (2001).
[14] T. Miyake, F. Aryasetiawan, T. Kotani, M. van Schilfgaarde, M. Usuda, and K. Terakura, Phys. Rev. B **66**, 245103 (2002).
[15] L. Schimka, J. Harl, A. Stroppa, A. Grüneis, M. Marsman, F. Mittendorfer, and G. Kresse, Nat. Mater. **9**, 741 (2010).
[16] M. Rohlfing and T. Bredow, Phys. Rev. Lett. **101**, 266106 (2008).
[17] X. Ren, P. Rinke, and M. Scheffler, Phys. Rev. B **80**, 045402 (2009).
[18] X. Ren, P. Rinke, C. Joas, and M. Scheffler, J. Mater. Sci. **47**, 7447 (2012).
[19] D. Lu, Y. Li, D. Rocca, and G. Galli, Phys. Rev. Lett. **102**, 206411 (2009).
[20] A. Marini, P. García-González, and A. Rubio, Phys. Rev. Lett. **96**, 136404 (2006).
[21] S. Lebègue, J. Harl, T. Gould, J. G. Ángyán, G. Kresse, and J. F. Dobson, Phys. Rev. Lett. **105**, 196401 (2010).
[22] T. Olsen, J. Yan, J. J. Mortensen, and K. S. Thygesen, Phys. Rev. Lett. **107**, 156401 (2011).
[23] M. Hellgren, D. R. Rohr, and E. K. U. Gross, J. Chem. Phys. **136**, 034106 (2012).
[24] J. Yan, J. J. Mortensen, K. W. Jacobsen, and K. S. Thygesen, Phys. Rev. B **83**, 245122 (2011).
[25] T. Olsen and K. S. Thygesen (2012), arXiv:1211.6873.
[26] X. Ren, A. Tkatchenko, P. Rinke, and M. Scheffler, Phys. Rev. Lett. **106**, 153003 (2011).
[27] K. M. Glassford and J. R. Chelikowsky, Phys. Rev. B **47**, 1732 (1993).
[28] Computational Materials Science **50**, 2295 (2011), ISSN 09270256.
[29] S. P. Ong, A. Jain, G. Hautier, M. Kocher, S. Cholia, D. Gunter, D. Bailey, D. Skinner, K. A. Persson, and G. Ceder, *The Materials Project* (2011), URL `http://materialsproject.org/`.
[30] V. Stevanović, S. Lany, X. Zhang, and A. Zunger, Phys. Rev. B **85**, 115104 (2012).
[31] M. W. Chase, *NIST-JANAF Thermochemical Tables* (American Chemical Society, New York, 1998).
[32] J. Harl and G. Kresse, Phys. Rev. B **77**, 045136 (2008).
[33] J. J. Mortensen, L. B. Hansen, and K. W. Jacobsen, Phys. Rev. B **71**, 035109 (2005).
[34] J. Enkovaara, C. Rostgaard, J. J. Mortensen, J. Chen, M. Dułak, L. Ferrighi, J. Gavnholt, C. Glinsvad, V. Haikola, H. A. Hansen, et al., J. Phys.: Condens. Matter **22**, 253202 (2010).
[35] A. Sorouri, W. M. C. Foulkes, and N. D. M. Hine, J. Chem. Phys **124**, 064105 (2006).
[36] C. Rostgaard, K. W. Jacobsen, and K. S. Thygesen, Phys. Rev. B **81**, 085103 (2010).
[37] R. H. Snow, *Thermodynamic Evaluation of the Possibility of Lithium Superoxide Production* (Defense Technical Information Center, 1965).
[38] R. H. Lamoreaux and D. L. Hildenbrand, J. Phys. Chem. Ref. Data **13**, 151 (1984).
[39] D. R. Lide, *CRC Handbook of Chemistry and Physics, 83rd Edition* (CRC Press, 2002).
[40] H. A. Wriedt, J. Phase Equilibria **6**, 337 (1985).
[41] The ZPE contribution to the formation energies in eV: Li_2O (0.13), Li_2O_2 (0.04), LiO_2 (0.01), Na_2O (0.02), Na_2O_2 (0.04), NaO_2 (0.02), K_2O (-0.04), K_2O_2 (-0.01), KO_2 (-0.02), Rb_2O (0.05), Rb_2O_2 (-0.02), RbO_2 (-0.01), Cs_2O (-0.04), Cs_2O_2 (-0.02), CsO_2 (0.01), BeO (-0.02), MgO (-0.07), CaO (-0.10), CaO_2 (-0.01), SrO (-0.04), BaO (-0.07), TiO_2 (0.00), RuO_2 (-0.01). The MAEs for both PBE and RPA calculations change by at most 0.01 eV by excluding the ZPEs, and the conclusions in this paper are not affected by ZPEs.
[42] Private discussions with Marcin Dułak.